Identification of Residues of FpvA Involved in the Different Steps of Pvd−Fe Uptake in *Pseudomonas aeruginosa*†

Mirella Nader,‡ Wim Dobbelaere,‡ Michel Vincent,§ Laure Journet,‡ Hendrik Adams,‡ David Cobessi,‡ Jacques Gallay,§ and Isabelle J. Schalk*,‡

Métaux et Microorganismes: Chimie, Biologie et Applications, UMR 7175-LC1 Institut Gilbert-Laustriat, CNRS and University Louis Pasteur, ESBS, F-67413 Illkirch, Strasbourg, France, CNRS UMR8619 IBBMC and Université Paris-Sud, Orsay, F-91405, France

Received May 23, 2007; Revised Manuscript Received August 1, 2007

ABSTRACT: FpvA is an outer membrane transporter involved in iron uptake by the siderophore pyoverdine (Pvd) in *Pseudomonas aeruginosa*. This transporter, like all other proteins of the same family, consists of a transmembrane 22 β-stranded barrel occluded by a plug domain. The β-strands of the barrel are connected by large extracellular loops and short periplasmic turns. Site-directed mutagenesis was carried out on FpvA to identify the extracellular loops or parts of these loops involved in the various stages of Pvd−Fe uptake. The G286C, W362C, and W434C mutations in loops L_1, L_3, and L_4, respectively, disturbed the binding of the apo siderophore, as shown by time-resolved fluorescence spectroscopy. Iron uptake experiments followed by fluorescence resonance energy transfer (FRET) or using ^{55}Fe indicated that residues W434 and G701 and, therefore, loops L_4 and L_9 must be involved in Pvd−Fe uptake by FpvA. The two corresponding mutants incorporated smaller than normal amounts of ^{55}Fe into cells, and no Pvd recycling on FpvA was observed after iron release. Surprisingly, the S603C mutation in loop L7 increased the amount of Pvd−Fe transported. Our results suggest that W434 (L_4), S603 (L_7), and G701 (L_9) are involved in the mechanism of Pvd−Fe uptake.

Iron is an essential element in all living organisms. Its uptake often requires the production of siderophores—low-molecular mass, high-affinity iron-chelating molecules—in Gram-negative bacteria (*1*−*3*). Siderophores facilitate iron solubilization and transport in the conditions of iron limitation prevailing in animal and plant hosts during infection. Iron uptake via siderophores in Gram-negative bacteria always involves a specific outer membrane transporter (OMT[1]) and an ABC transporter for transport across the outer and inner membranes, respectively (*3*). The energy required for transport across the inner membrane is provided by ATP hydrolysis. The protonmotive force of the inner membrane drives OMT-mediated transport across the outer membrane by means of an inner membrane complex comprising TonB, ExbB, and ExbD (*4*, *5*).

Under conditions of iron limitation, pyoverdine (Pvd, Figure 1) is one of the major siderophores produced by *Pseudomonas aeruginosa*. This molecule possesses a chromophore derived from 2,3-diamino-6,7-dihydroxyquinoline that renders the molecule colored and fluorescent and is linked to a partly cyclic octapeptide (*6*, *7*). Iron(III) is chelated by the catecholate group of the quinoline moiety and the two hydroxamate groups of the two δ-*N*-hydroxy-ornithines of the octapeptide, with an association constant of approximately 10^{32} M^{-1} at neutral pH (*8*). Pvd−Fe is recognized at the outer membrane and transported into the periplasm by the specific OMT, FpvA. The structures of FpvA bound to Pvd and Pvd−Fe have been solved (*9*, *10*). This protein, like all siderophore outer membrane transporters, folds into two domains: a transmembrane β-barrel of 22 antiparallel β-strands filled by a small domain, known as the plug domain. The β-strands of the barrel are connected by long extracellular loops and short periplasmic turns. The Pvd−Fe binding site is located at the top of the β-barrel and is composed mostly of aromatic residues from the plug and β-barrel domains. This site is able to bind with close affinities the apo and the ferric-form of the siderophores (K_i = 6.8 nM and 0.5 nM respectively) (*11*).

In the absence of environmental iron, large amounts of Pvd are produced by *P. aeruginosa* (200 mg/L in succinate medium at 29 °C). Since FpvA is able to bind both Pvd and Pvd−Fe, most of the FpvA transporters at the cell surface are loaded with apo-Pvd, under iron limitation. Therefore, the first step for Pvd−Fe uptake involves the exchange of metal-free bound Pvd for Pvd−Fe on FpvA (*12*). The Pvd−

† This work was partly funded by the Centre National de la Recherche Scientifique, the Association Vaincre la Mucoviscidose (French Association against Cystic Fibrosis), and a grant from the ANR (Agence Nationale de Recherche, ANR-05-JCJC-0181-01). L.J. was supported by an EMBO postdoctoral fellowship.

* Corresponding author. Métaux et Microorganismes: Chimie, Biologie et Applications, UMR 7175-LC1 Institut Gilbert-Laustriat, ESBS, Blvd Sébastien Brandt, BP 10412, F-67413 Illkirch, Strasbourg, France. Tel: 33 3 90 24 47 19. Fax: 33 3 90 24 48 29. E-mail: schalk@esbs.u-strasbg.fr.

‡ UMR 7175-LC1 Institut Gilbert-Laustriat, CNRS and University Louis Pasteur, ESBS.

§ CNRS UMR8619 IBBMC and Université Paris-Sud.

[1] Abbreviations: Pvd and Pvd−Fe, iron-free and ferric pyoverdine, respectively, produced by *Pseudomonas aeruginosa 15692*; FpvA, Pvd outer membrane receptor; FRET, fluorescence resonance energy transfer; KI, potassium iodide; OMT, outer membrane transporter.

10.1021/bi700997w CCC: $37.00
Published on Web 09/27/2007

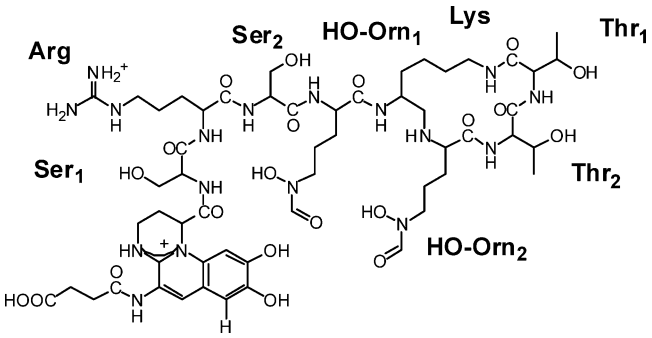

FIGURE 1: Pvd structure.

Fe complex is then transported into the periplasm and iron is released from the siderophore by a process involving iron reduction (*13*). Both the Pvd/Pvd−Fe exchange on FpvA and ferric-siderophore uptake across the outer membrane are dependent on protonmotive force (pmf) and TonB (*11*). Finally, after iron release, free Pvd is excreted in the extracellular medium and binds again to FpvA (*14*). The transporter and the mechanism involved in this Pvd recycling in the extracellular medium are so far unknown.

The translocation of Pvd−Fe across the outer membrane by FpvA is itself a multistep process. The structures of unloaded FecA (the dicitrate−Fe OMT in *Escherichia coli*) and FecA loaded with apo- and ferric-siderophore (*15*, *16*), functional studies on FepA (the enterobactin−Fe OMT in *E. coli*) (*17*−*19*) and on FhuA (*20*), and time-resolved fluorescence spectroscopy studies on FpvA (*21*), have suggested that two gating processes control uptake. The first gate consists of the extracellular loops closing over the binding site after the binding of siderophore−Fe, and the second consists of the plug closing the barrel and access to the periplasm.

The opening of the second gate involves a change in the conformation of the periplasmic N-terminal region of the transporter (the TonB box), indicating to the TonB machinery that the OMT is loaded with a siderophore−Fe complex and ready for uptake (*5*). The interaction between the OMT and the TonB machinery must induce a major change in the conformation of the transporter, opening a channel (second gate). It was initially thought that there were too many interactions between the plug and the inner face of the barrel for complete removal of the plug from the barrel. However, recent single-molecule unfolding experiments in the context of OMTs have suggested that TonB, by exerting a very modest mechanical force upon the OMT, could drive large conformational changes or unfolding of the plug domain during siderophore−Fe uptake (*22*). Moreover, in all OMT structures, the plug domain is highly solvated by water molecules within the barrel. These solvating water molecules may function as a lubricant, decreasing the energetic cost of the movement of the plug within the barrel (*23*). At last, a residue on the normally buried surface of the N-domain of FepA was recently labeled by fluorescein maleimide in the periplasm, providing evidence that the transport process involves expulsion of the globular domain from the β-barrel (*24*).

Binding and iron uptake assays with Pvd analogues have shown that the opening of the second gate results in the formation of a large channel, because the succinyl moiety linked to the chromophore of Pvd and the first amino acid of the peptide moiety can be sterically hindered by aryl azide groups, with no effect on the binding or iron uptake properties of Pvd−Fe (*25*).

FpvA also plays a critical role in controlling the expression of *fpvA* and genes related to Pvd biosynthesis, by a regulation cascade (*26*). This cascade involves a transmembrane signaling system induced by the binding of the siderophore(−Fe) to the OMT, and the extracytoplasmic function (ECF) sigma factor/antisigma factor pairs, FpvI/FpvR and PvdS/FpvR (*26*−*33*). This regulation resembles PupIR control of the PupB pseudobactin−Fe receptor in *Pseudomonas putida* and FecIR control of the FecA dicitrate−Fe OMT, FecA in *E. coli* (*34*−*36*). Following siderophore binding by the FpvA receptor, a signal is transmitted to the antisigma factor FpvR, resulting in activation of the FpvI and PvdS sigma factors (*27*−*30*). PvdS directs the transcription of Pvd synthesis genes, in addition to those encoding some secreted enzymes, and FpvI recognizes the promoter of the gene encoding FpvA. However, it is still not clear whether the signaling molecule is Pvd−Fe or apo-Pvd.

Several mutations have been introduced into FpvA extracellular loops, for studies of the involvement of these loops in various stages of Pvd−Fe uptake across the outer membrane: (i) binding of the siderophore to FpvA, (ii) movements of the extracellular loops (first gate) of FpvA after binding to Pvd−Fe, (iii) opening of the second gate (plug domain), and (iv) Pvd recycling on FpvA after the release of iron into the periplasm. We used various techniques (time-resolved fluorescence spectroscopy, FRET, Pvd−^{55}Fe uptake) to study the phenotypes of these mutants. Mutations G286C (loop L_1), W362C (loop L_3), and W434C (loop L_4) affected the binding of the metal-free siderophore to FpvA, and mutations W434C, S603C, and G701C affected the Pvd−Fe transport and Pvd production. The FpvAW434C and FpvAG701C mutations decreased the amount of Pvd−^{55}Fe incorporated into the cells whereas FpvAS603C increased the amount incorporated, using the wild-type strain as a reference.

MATERIALS AND METHODS

Bacterial Strains, Plasmids, and Growth Media. All enzymes for DNA manipulation were purchased from Fermentas and used according to the manufacturer's instructions. *Escherichia coli* strain TOP10 (Invitrogen) was used as a host strain for all plasmid constructions. Site-directed mutagenesis was facilitated by amplifying the *fpvA* gene by PCR, using *Pfx* polymerase (Invitrogen) and pPVR2 (*37*), which carries the *fpvA* gene on a 4.6 kb *Sph*I fragment, as a template. The primers used were AEI255 (5′-GGATCCACACCGGCCGCATCAGCGAAACCGCGAACAACATCC-3′) and AEI256 (5′-AAGCTTATCGAGGGGCAGGCGCGTGAGTCGTTGCTGCTC-3′), which contain a *Bam*HI and *Hin*dIII site (both underlined), respectively. Primer AE255 binds 1099 bp upstream from the ATG start codon, and primer AE256 binds 1042 bp downstream from the TAA stop codon. The resulting 4.6-kb PCR product was inserted into pCR4Blunt-TOPO (Invitrogen) according to the manufacturer's instructions, resulting in pTOPO-FpvA.

Mutagenesis was carried out with the QuickChange XL Site-Directed Mutagenesis Kit (Stratagene), according to the

manufacturer's instructions, using pTOPO-FpvA as the template. The oligonucleotides used for site-specific mutagenesis are the following: 5′-GTCGAACTGGGCGC*GT*GCAGTTGGGACAATTAC-3′ for G286C mutant, 5′-CCCAAGGGATCGGG*CTGCAGC*GGCAGCTTCCCG-3′ for W362C mutant, 5′-GCGATCATGGGCGACTG*T*C*CT*GCACCGGACAAC-3′ for W434C mutant, 5′-AGTTGGTATCGCGAC*T*GCAGCAACAAGCTGCTC-3′ for S603C mutant, and 5′-GACCTACTACACCAA*CATATG*TTTCTACACCTCGGCATCC-3′ for G794C mutant (mutated DNA bases are shown in italics). Cysteine mutagenesis was accompanied by the introduction of silent base modifications, resulting in novel restriction sites (underlined) to facilitate screening for the correct mutations. All mutations were confirmed by sequence analysis. The mutant FpvA proteins were produced in *P. aeruginosa*, by excising the mutated *fpvA* genes from the pTOPO-FpvA vectors with *Bam*HI and *Hin*dIII, and ligating them into the corresponding sites of pMMB190 (*38*), yielding pMMB-FpvA(mut) (where mut denotes the mutation). These plasmids were transferred by conjugation into the Δ*fpvA* mutant K437 (*39*), using pRK2013 as a helper plasmid (*40*).

The iron-deficient succinate minimal medium used in these studies has been described elsewhere (*6*). LB broth (Lennox) and LB broth agar medium were used as rich medium in all experiments; both were purchased from Difco. All media were supplemented with the relevant antibiotics at the following concentrations: tetracycline (50 μg/mL), carbenicillin (150 μg/mL), and ampicillin (100 μg /mL).

Pvd Production. The strains were grown overnight in succinate medium (*6*) at 29 °C. The amount of Pvd produced was estimated by monitoring absorbance at 400 nm in the extracellular medium, using the extinction coefficient of Pvd ($\epsilon = 19000\ M^{-1}$).

^{55}Fe Uptake in P. aeruginosa ATCC 15692. ^{55}Fe uptake assays with the various mutants of FpvA were carried out as previously described (*41*). The cells were prepared at an optical density at 600 nm of 0.5 in 50 mM Tris-HCl (pH 8.0). The final concentrations of Pvd−[^{55}Fe] complex were 0.5 μM. The mixtures were stirred at 29 °C during 30 min and filtered afterward on 0.45 μm porosity filters (Microsep, France), presoaked in a 0.1% solution of polyethyleneimine. Each filter was rapidly washed twice with 3 × 2 mL of Tris-HCl 50 mM pH 8.0 and the radioactivity counted.

Steady-State Fluorescence Spectroscopy. Fluorescence resonance energy transfer (FRET) experiments were performed with a PTI (Photon Technology International Time-Master, Bioritech) spectrofluorometer. In all experiments, the sample was stirred at 29 °C in a 1 mL cuvette, the excitation wavelength was set at 290 nm, and fluorescence emission was measured at 447 nm. We studied the kinetics of iron uptake, as previously described (*11*, *12*, *21*). The cells were grown overnight as described above at an optical density at 600 nm of 0.5−0.7. The cells were then pelleted, washed 4 times with an equal volume of fresh medium, and resuspended in 50 mM Tris-HCl (pH 8.0) at an optical density at 600 nm of 2. The bacterial suspension (995 μL) was stirred at 29 °C in a 1 mL cuvette. Five microliters of ferric-Pvd was added to the 995 μL of bacterial solution, to obtain a final concentration of 0.3 or 0.6 μM ferric-Pvd. The decrease in fluorescence at 447 nm (excitation set at 290 nm) was measured every second. The same experiment was repeated in the absence of ferric-Pvd.

For the experiments carried out in the presence of urea, purified FpvA receptors were incubated in 50 mM Tris-HCl pH 8.0, 1% octyl-POE and in the presence of increasing concentrations of urea for 1 h. The excitation wavelength was set at 290 nm, and fluorescence emission was measured from 310 to 550 nm.

Time-Resolved Fluorescence Measurements. Fluorescence intensity and anisotropy decays of Pvd bound to the purified wild-type FpvA and its mutants were obtained from the polarized components $I_{vv}(t)$ and $I_{vh}(t)$ by the time-correlated single-photon counting technique. We used a blue diode laser LDH400 (maximum emission at 392 nm) from Picoquant (Berlin-Adlershof, Germany), operated at 10 MHz. The fluorescence emission wavelength was selected with a single monochromator (Jobin Yvon UV-H10, bandwidth 8 nm). A Hamamatsu fast photomultiplier (model R3235-01) was used for detection. The instrument response function (∼500 ps) was monitored using a sample scattering at the emission wavelength. Time resolution was ∼20 ps. Each experimental decay $I_{vv}(t)$ and $I_{vh}(t)$ was stored on a 2K plug-in multichannel analyzer card (Orter Trup-PCI 2k, Ametek France), using Maestro-32 software. Data were sampled automatically, under microcomputer control. The instrumental response function was evaluated automatically every 5 min, by measuring the scattering of a glycogen solution over a 30 s period at the excitation wavelength, alternating for 90 s with the parallel and perpendicular components of the polarized fluorescence decay, until a total of several million counts had been reached for fluorescence intensity decay. Samples were contained in microcuvettes (120 μL).

Fluorescence intensity decay was analyzed as a sum of exponentials, $I(t) = \sum \alpha_i \exp(-t/\tau_i)$, where α_i is the normalized amplitude and τ_i the lifetime of intensity decay, by the maximum entropy method. MEMSYS 5 (MEDC Ltd., U.K.) was used as a library of subroutines. Sets of 150 lifetime values, equally spaced on a log scale, were used. Fluorescence anisotropy decays were analyzed classically as a sum of exponential terms $A(t) = \sum \beta_i \exp(-t/\theta_i)$ where β_i is the anisotropy and θ_i the rotational correlation time. Sets of 100 correlation time values, equally spaced on a log scale, were used. For the experiments in the presence of KI, a stock solution of 5 M KI containing 0.1 mM $Na_2S_2O_3$ was used.

RESULTS

Site-Directed Mutagenesis of fpvA and Insertion of Mutant Proteins into the Outer Membrane. We investigated the molecular mechanisms involved in the biological functions of this transporter by introducing a set of six unique single cysteine mutations, all located in the extracellular loops, into FpvA (Figure 2). The mutated residues were chosen before the FpvA structures were solved, based on sequence alignment with FhuA and using the FhuA structure. Only one of these mutations involved a residue of the Pvd or Pvd−Fe binding site (W362C). Cys mutations were introduced in order to label these residues in a next step, with fluorescent probes or spin markers (EPR studies) for further investigation.

The cysteine FpvA mutant sequences were inserted into the broad-host range expression vector pMMB190 and

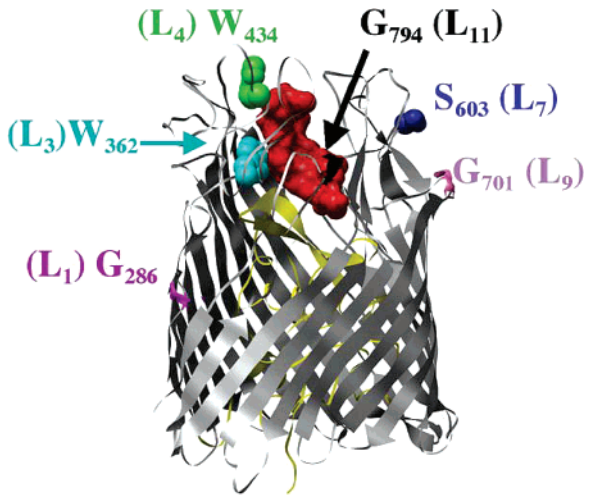

FIGURE 2: Crystal structure of FpvA at 3.6 Å, highlighting (in spacefill to assist visualization) the mutated residues in the extracellular loops. The β-barrel and the plug domains of FpvA are colored respectively in gray and in yellow, and the siderophore Pvd is colored in red.

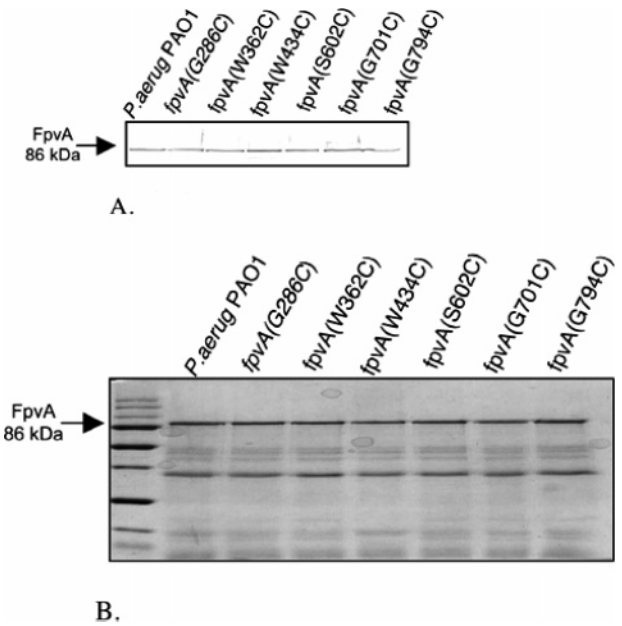

FIGURE 3: Expression and localization of the different FpvA mutants. A. Immunoblot analyses of total cell. Cells from strains *P. aeruginosa* PAO1, K437 (Δ*fpvA*), and K437 harboring plasmids pMMB190 with the mutated *fpvA* gene were cultured overnight in iron-deficient succinate medium and analyzed by SDS−PAGE followed by Western blotting and immunodetection using polyclonal FpvA-specific antiserum. B. Coomassie stained SDS−PAGE of outer membrane proteins prepared from cells of *P. aeruginosa* PAO1, K437 (Δ*fpvA*), and K437 harboring plasmids pMMB190 with the mutated *fpvA* gene. The position of FpvA is indicated with an arrow.

transferred to Δ*fpvA* K437 strain. In these constructs, the various *fpvA* mutants were under the control of their own promoter, and their expression was thus induced in iron-limited conditions. Outer membranes isolated from all these cells were analyzed for FpvA levels and distribution, by SDS−PAGE and Western blotting (Figure 3). FpvA levels were similar to or higher than those in the wild-type strain PAO1, and the mutated transporter was correctly targeted to the outer membrane. Cell growth was not affected by these mutations (data not shown). When pMMB190 constructs encoding these cloned receptors were transferred into a Δ*fpvA* ΔPvd strain, no detectable expression of FpvA was observed unless Pvd was added to the medium (data not shown).

In order to evaluate the effect of the mutation on the stability of FpvA, purified receptors were incubated in the presence of increasing concentrations of urea and the fluorescence of Trps was monitored (Figure 4). The fluorescence of Trp residues depends on the environment of the residue. If during denaturation a Trp residue leaves the hydrophobic core of the protein and is exposed to water, both the wavelength and the intensity of the fluorescence will be changed. Denaturation of the protein started with 4 M urea for wild-type FpvA and for all the mutants except FpvA(W362C) and FpvA(G701C), which were apparently slightly more stable (denaturation started with 6 M urea) (Figure 4B). None of the mutations introduced in FpvA had a dramatic effect on the protein stability.

Effects of the Mutation on Iron-Free Pvd Binding. In conditions of iron limitation, large amounts of Pvd are produced by *P. aeruginosa* strains (200 mg/L). Since FpvA is able to bind metal-free Pvd with an affinity of 7 nM, apparently all FpvA receptors at the cell surface are loaded with metal-free Pvd in the absence of iron (*12*, *42*). The purified FpvA−Pvd complex has been characterized by time-resolved fluorescence spectroscopy (*21*). We used this technique here to study the effect of the mutations on the ability of purified FpvA to bind and interact with metal-free Pvd. The fluorescence properties of Pvd in its binding site (Table 1), its mobility (Table 2) and accessibility to the solvent (Table 3) were compared, for each of the six mutations, with the data previously obtained with the wild-type purified FpvA−Pvd complex (*21*).

Only three (FpvA(G286C), FpvA(W362C), and FpvA-(W434C)) of the six mutations affected the Pvd-binding properties of the transporter (Table 1−3). For FpvA(W362C), a mutation in the close neighborhood of Pvd, the fluorescence intensity decay of the chromophore became more heterogeneous, with an additional short lifetime compared to the wild type (Table 1). We previously showed (*21*) that the Pvd fluorescence intensity decay was sensitive to pH which affected the protonation state of the catechol group. We suggested, according to the similarity between the Pvd fluorescence decays at pH 4 and bound to FpvA, that the catechol of Pvd bound to FpvA was either protonated or H-bonded to protein groups of the binding site. In agreement with this hypothesis, the 3D structure of the FpvA−Pvd complex showed later on that the OH functional group of the catechol was in fact H-bonded to the side chain of Arg204 and Tyr796 (*9*). The pattern of the fluorescence intensity decay of Pvd bound to the W362C mutant suggested a larger heterogeneity of H-bonded states of the Pvd chromophore in the mutant, compared to its full H-bonded state in the wild-type receptor. The replacement of the W362 indole side-chain with the less bulky cysteine thiol group provokes likely changes in orientation and/or distances of the amino acid side-chains in interaction with the Pvd catechol. This mutation affects also the fluorescence anisotropy decay which reveals a larger mobility of Pvd in the FpvA(W362C)−Pvd complex characterized by a faster rotational correlation time and a larger semi-angle of rotation compared to FpvA−Pvd

Table 1: Time-Resolved Fluorescence Emission Parameters (Excited-State Lifetime τ_i and Their Amplitudes α_i) of Pvd Bound to FpvA or Mutated FpvA[a]

sample	τ_1 (ns)	τ_2 (ns)	τ_3 (ns)	τ_4 (ns)	α_1	α_2	α_3	α_4	$\langle\tau\rangle$ (ns)
FpvA	6.89 ± 0.03		1.86 ± 0.19	0.26 ± 0.11	0.66 ± 0.08		0.11 ± 0.04	0.26 ± 0.12	4.65 ± 0.67
FpvA(G286C)	6.99 ± 0.04		2.28 ± 0.96	0.60 ± 0.30	0.58 ± 0.02		0.17 ± 0.02	0.25 ± 0.01	4.57 ± 0.35
FpvA(W362C)	6.87 ± 0.09	2.56 ± 0.39	0.73 ± 0.14	0.17 ± 0.01	0.44 ± 0.07	0.11 ± 0.04	0.24 ± 0.02	0.22 ± 0.12	3.32 ± 0.29
FpvA(W434C)	6.66 ± 0.17		1.37 ± 0.10	0.20 ± 0.01	0.65 ± 0.01		0.26 ± 0.03	0.09 ± 0.01	4.71 ± 0.12
FpvA(S603C)	6.76 ± 0.03		1.69 ± 0.07	0.18 ± 0.02	0.66 ± 0.03		0.07 ± 0.01	0.27 ± 0.04	4.60 ± 024
FpvA(G701)	6.73 ± 0.01		1.84 ± 0.01	0.18 ± 0.01	0.61 ± 0.01		0.08 ± 0.01	0.31 ± 0.01	4.30 ± 0.01
FpvA(G794C)	6.72 ± 0.02		1.84 ± 0.19	0.16 ± 0.01	0.56 ± 0.02		0.06 ± 0.01	0.38 ± 0.02	3.90 ± 0.15

[a] MEM analysis was performed on the fluorescence intensity $S(t)$ reconstructed from the parallel and perpendicular polarized components $I_{vv}(t)$ and $I_{vh}(t)$ such as $S(t) = I_{vv}(t) + 2GI_{vh}(t) = \int_0^\infty \alpha_i(\tau_i) \exp(-t/\tau_i)\, d\tau$, where τ_i is the excited-state lifetime, $\alpha_i(\tau_i)$ is its normalized amplitude distribution, and G is a correction factor accounting for the difference in transmission of the $I_{vv}(t)$ and $I_{vh}(t)$ components. The mean lifetime $\langle\tau\rangle$ is calculated as $\langle\tau\rangle = \sum_i \alpha_i\tau_i$. Standard deviations for 3−4 measurements are shown. Excitation wavelength: 392 nm. Emission wavelength: 450 nm.

Table 2: Fluorescence Anisotropy Decay Parameters of Pvd Bound to FpvA or Mutated FpvA[a]

sample	θ_1 (ns)	θ_2 (ns)	β_1	β_2	ω_{max} (deg)
FpvA	3.4 ± 1.9	116 ± 15	0.003 ± 0.003	0.373 ± 0.009	11 ± 2
FpvA(G286C)	0.6 ± 0.2	99 ± 3	0.022 ± 0.007	0.311 ± 0.09	20 ± 4
FpvA(W362C)	0.38 ± 0.02	116 ± 4	0.043 ± 0.005	0.276 ± 0.007	28 ± 1
FpvA(W434C)	0.45 ± 0.01	134 ± 3	0.049 ± 0.008	0.298 ± 0.003	25 ± 1
FpvA(S603C)	1.1 ± 0.5	136 ± 6	0.016 ± 0.004	0.387 ± 0.003	9 ± 2
FpvA(G701C)	0.8 ± 0.4	142 ± 3	0.018 ± 0.02	0.388 ± 0.006	8 ± 2
FpvA(G794C)	0.7 ± 0.4	141 ± 15	0.018 ± 0.006	0.377 ± 0.005	11 ± 1

[a] The fluorescence anisotropy is assumed to be described by a sum of exponentials: $r(t) = [I_{vv}(t) - GI_{vh}(t)]/[I_{vv}(t) + 2GI_{vh}(t)] = \sum_i \beta_i \exp(-t/\theta_i)$. G is a correction factor accounting for the difference in transmission of the $I_{vv}(t)$ and $I_{vh}(t)$ components. The θ_i and β_i coefficients are respectively the values of the center and partial anisotropy of each rotational correlation time peak. The wobbling-in-cone angle ω_{max} was calculated from $[\beta_2/r_0] = [(1/2)\cos\omega_{max}(1 + \cos\omega_{max})]^2$ (*47*), using a value of the intrinsic anisotropy r_0 of 0.394, measured in vitrified medium (glycerol 75% w/w at −50 °C) (*21*). Excitation wavelength: 392 nm. Emission wavelength: 450 nm.

Table 3: Stern−Volmer Iodide Quenching Parameters[a]

sample	K_{SV} (M^{-1})	τ (ns)	k_q (s)
Pvd pH 4	1.93	6.22	3×10^8
FpvA	0.26	6.85	4×10^7
FpvA(G286C)	0.70	6.99	1×10^8
FpvA(W362C)	0.57	6.87	8×10^7
FpvA(W434C)	0.55	6.79	8×10^7

[a] K_{sv} is the Stern−Volmer constant given by the slope of the linear plot τ_1/τ versus $[I^-]$ (τ_1 and τ are the excited-state lifetime values in the absence and in the presence of I^- respectively. k_q is the bimolecular quenching constant: $k_q = K_{sv}/\tau_1$. Excitation wavelength: 392 nm. Emission wavelength: 450 nm.

(Table 2). This mutation induces also a higher accessibility of Pvd to the solvent, assessed by a value of the bimolecular quenching constant k_q of iodide twice as high in this mutant as in the wild-type receptor (Table 3). In FpvA−Pvd, W362 is close to a hydroxamate group of the Pvd octapeptide moiety, and may therefore be involved in FpvA−Pvd stabilization.

W434 is located in loop L_4, ~10 Å from the Pvd molecule, and contributes to loop stability through van der Waals interactions with the surrounding residues of loop L_4. Consistent with the large distance between the mutation and the fluorophore in the FpvA(W434C) mutant, the interactions of the catechol with the groups stabilizing the Pvd molecule in the receptor binding site are almost unaffected as assessed by the slight change in Pvd fluorescence intensity decay: a greater contribution of the intermediate lifetime and a lesser contribution of the shortest lifetime were generally observed (Table 1). The influence of this mutation on the mobility of the bound Pvd was, however, far from negligible, as shown by the doubling of the semi-angle of the wobbling-in-cone subnanosecond motion ω_{max} with respect to the wild-type receptor (Table 2). The accessibility of Pvd to the solvent was also greater for this mutant than for the wild type, as shown by the higher bimolecular quenching constant for iodide (Table 3). A larger opening of the Pvd binding site is likely in this FpvA(W434C) mutant.

G286 is located at the C-terminal end of β-strand $\beta1$ of the β-barrel, far from the Pvd binding site. The fluorescence intensity decay of the chromophore was not affected in FpvA(G286C) (Table 1), indicating that the major interactions of the fluorescent ring, and of the catechol group in particular, are preserved in this mutant, whereas they are not in the W362C mutant. However, fluorescence anisotropy decay and accessibility to the water-soluble quencher KI with this mutant differed from those for the wild-type FpvA−Pvd complex. In this mutant, Pvd was significantly more mobile in its binding site, as shown by the higher value of the semi-angle ω_{max} of the wobbling-in-cone rotation (Table 2). It was also more solvent-accessible, as shown by the higher value of the bimolecular quenching constant in these mutants than in the wild-type transporter (Table 3).

For the other three mutations in the extracellular loops (FpvA(S603C), FpvA(G701C), and FpvA(G794C)), no significant change in fluorescence intensity decay or anisotropy decay was observed (Tables 1 and 2).

Effects of the Mutations on Pvd−Fe Uptake. We investigated the iron-transporting abilities of the six mutants, using either ^{55}Fe or FRET. The relative amounts of ^{55}Fe acquired by the cells were compared (Figure 5). FpvA(G286C), FpvA(W362C), and FpvA(G794C) transported similar amounts of iron to the wild-type FpvA over the 30 min incubation period. FpvA(W434C) (loop L_4) and FpvA(G701C) (loop

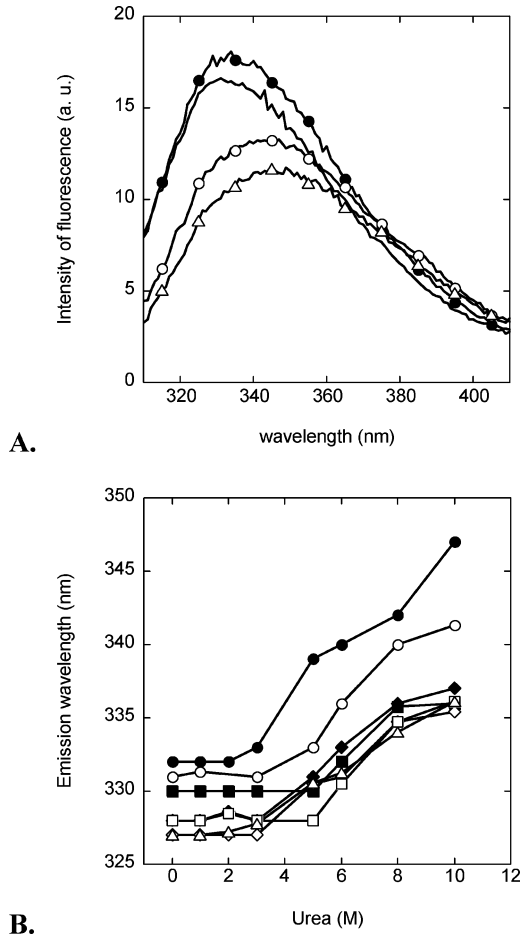

FIGURE 4: A. Evolution of the intrinsic Trp emission spectrum of wild-type FpvA as a function of urea concentration (0 M urea (black line), 1 M urea (●), 8 M urea (○) and 10 M urea (△)). B. Evolution of the intrinsic Trp emission of fluorescence for all the mutants as a function of urea concentration. The experiment has been carried out with wild-type FpvA (●), FpvA(G286C) (◆), FpvA(W362C) (■), FpvA(W434C) (○), FpvA(S603C) (◇), FpvA(G701C) (□), FpvA(G794C) (△). Purified FpvA and mutants (100 μg/mL) were incubated in 50 mM TrisHCl pH 8.0, 1% octyl-POE and in the presence of increasing concentrations of urea (0 to 10 M). The excitation wavelength was set at 290 nm.

L_9) accumulated 20% and 60%, respectively, less ^{55}Fe than the wild type. In contrast, FpvA(S603C) (loop L_7) seemed to transport Pvd−Fe more efficiently than the wild type, as 70% more ^{55}Fe was incorporated.

We used FRET analysis, with the Trp residues of FpvA, to follow the complete Pvd−Fe uptake cycle in the mutants. The typical fluorescence signal for iron uptake via Pvd in *P. aeruginosa*, when excited at 290 nm and monitored at 447 nm, displays two steps: a decrease of fluorescence corresponding to the formation of FpvA−Pvd−Fe upon the addition of Pvd−Fe; and a subsequent increase corresponding to the recycling of Pvd on FpvA (formation of FpvA−Pvd_{recy}) (Figure 6A (*13*, *14*)). During the second step, the fluorescence always returned exactly to the same level as that before the addition of Pvd−Fe, indicating that all the FpvA receptors were loaded again with iron-free recycled Pvd. In the presence of saturating concentrations of Pvd−Fe, the time course is monophasic (Figure 6B), indicating that all of the receptors remained loaded with Pvd−Fe and that recycled or newly synthesized Pvd molecules were unable to bind to the receptor, probably because present at a lower concentration compared to Pvd−Fe (*14*). These typical FRET signals were observed for FpvA(W362C) and FpvA(G794C) (Figure 6B), indicating that these transporters, despite their mutation, could still undergo loading with Pvd−Fe, transporting this complex into the periplasm. The metal was then released and free Pvd was recycled on the transporters.

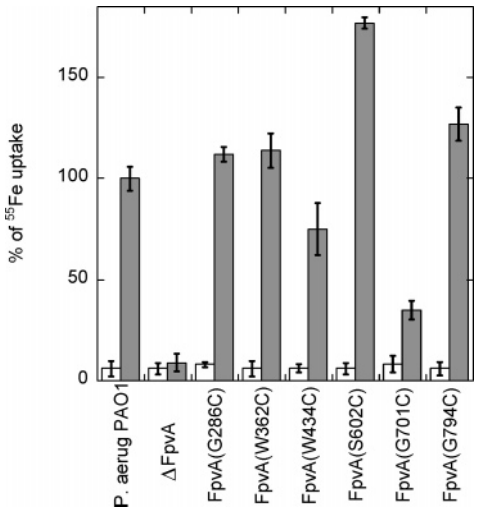

FIGURE 5: Pvd-mediated ^{55}Fe uptake by *P. aeruginosa* PAO1 and K437 (Δ*fpvA*) expressing mutant FpvA receptors. Cells cultured in the absence of iron were washed and resuspended at an OD_{600} of 0.6 in 50 mM Tris-HCl (pH 8.0) and incubated in the presence of 0.5 μM Pvd−^{55}Fe at 30 °C (white) and at 0 °C (black). Incubation was stopped after 30 min; the cells were washed and harvested on filters. Data are the means of triplicate experiments.

For FpvA(G286C) and FpvA(S603C) (Figure 6C), this signal was characterized by larger amplitudes for the fluorescence intensity of the recycling step than for the first step. As the amplitude of FpvA−Pvd−Fe formation (first step) was similar to that for formation of the equivalent complexes with FpvA(W362C) and FpvA(G794C) (Figure 6B), the larger amplitude of the second step may be due to more efficient FRET for FpvA−Pvd_{recy}, due to a more favorable conformation of the transporter.

Finally, a third type of fluorescent signal was observed for FpvA(G701C) and FpvA(W434C). Only the first part of the fluorescent signal, the decrease in fluorescence was observed (Figure 6D), indicating that these transporters were loaded with Pvd−Fe, but that no recycling occurred, even after 2 h (data not shown). This may be due to an FpvA transporter blocked in its Pvd−Fe-loaded form being unable to transport Pvd−Fe into the periplasm. Alternatively, Pvd−Fe may be transported into the periplasm and iron released from the siderophore, but the mutated transporter may not be able to recycle Pvd or to bind recycled Pvd. Moreover, the kinetics of FpvA−Pvd−Fe formation for FpvA(W434C) and FpvA(G701C) are slower than those for wild-type FpvA. Equilibrium was reached after more than an hour for FpvA-(W434C) and FpvA(G701C) (Figure 6D) and within 10 min for wild-type FpvA (*13*) and the other four mutants (Figures 6B and 6C). Moreover, for FpvA(W434C) and FpvA-(G701C), the binding trace was clearly a composite of at least two kinetics parameters, indicating that binding occurred in at least two steps. The first step is a rapid process, taking place in the course of a minute or so. It represents about half of the FRET and probably corresponds to the binding of Pvd−Fe to the transporter. The dependence on Pvd−Fe

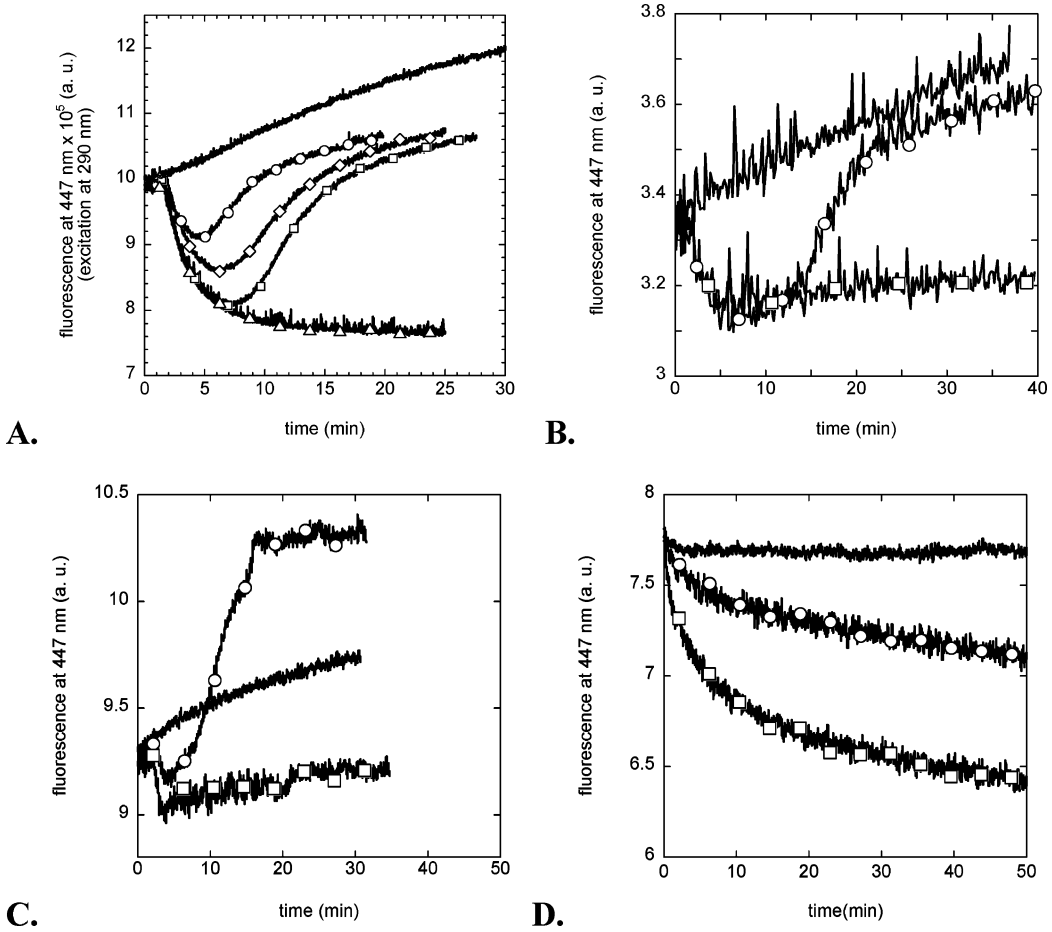

FIGURE 6: Iron uptake followed by FRET. Panel A shows the typical fluorescent signal obtained with strains expressing wild-type FpvA. The Pvd-producing, FpvA-overproducing K691(pPVR2) cells were washed and resuspended at an OD_{600} of 2 in 50 mM Tris-HCl (pH 8.0) and incubated at 29 °C. After the addition of 0 nM (black line), 25 nM (○), 50 nM (◇), 100 nM (□), 250 nM (△) of Pvd−Fe, the variation in fluorescence at 447 nm (excitation set at 290 nm) was monitored by measuring the emission of fluorescence at 447 nm every second for 30 min (*14*). Panels B, C, and D: Cells (*fpvA*(W362C), panel B; *fpvA*(G286C), panel C; *fpvA*(W434C), panel D) cultured in the absence of iron were washed and resuspended at an OD_{600} of 2 in 50 mM Tris-HCl (pH 8.0). We then added 300 nM (○, panels B, C, and D) or 600 nM Pvd−Fe (□, panels B, C, and D), and monitored changes in fluorescence at 447 nm (excitation at 290 nm). The experiments were repeated in the absence of cells (black line, panels B, C, and D). For the other three mutants, the observed kinetics were similar to those presented in panels B, C, and D for FpvA(G794C), FpvA(S603C), and FpvA(G701C), respectively.

concentration of this first step for FpvA(W434C) and FpvA-(G701C) indicates that these two mutants probably have a lower affinity for Pvd−Fe than wild-type FpvA. The second step took about half an hour, and its biological significance is unknown but may correspond to a change of conformation of the transporter. The data obtained for FpvA(W434C) and FpvA(G701C) are consistent with a simple kinetic pattern, involving the binding of Pvd−Fe to the FpvA receptor, followed by isomerization to stabilize the rate. A similar kinetic scheme has already been reported *in vitro* and *in vivo* for FpvA in the absence of TonB activation (*11*). However, the amplitude of the first kinetic component represented about 90% of the FRET signal in previous studies.

Effects of the Mutations on Pvd Production. In addition to transporting Pvd−Fe, FpvA also plays a critical role in controlling the expression of *fpvA* and of genes relating to Pvd biosynthesis, through a regulatory cascade (*26*). The G286C, W362C, and G794C mutants produced similar quantities of Pvd to the wild type. The W434C, S603C, and G701C mutants produced 20% less Pvd. This Pvd production was estimated using the absorbance of this siderophore at 400 nm (*8*).

DISCUSSION

We previously used the fluorescent properties of Pvd to investigate the mechanism of iron uptake by the FpvA/Pvd pathway. We used this approach again in this study, together with site-directed mutagenesis on FpvA. Six mutations were introduced into the extracellular loops of FpvA (Figure 2) to facilitate identification of the extracellular loops or parts of these loops involved in the various steps of Pvd−Fe uptake. None of the mutations affected the export of the transporter in the outer membranes (Figure 3) and its stability (Figure 4). Among the six mutations, only one mutation (G794C located on loop L_{11}) gave the wild-type phenotype for Pvd production, siderophore binding, and iron uptake (Table 4). This mutation had no apparent structural consequences for Pvd−Fe binding and transport, even though G794 was followed by Phe795 and Tyr796, both of which are involved in the Pvd binding pocket. The other five mutants had phenotypes different from that of the wild type (Table 4).

Metal-Free Pvd Binding. FpvA, like FptA (the pyochelin−Fe OMT in *P. aeruginosa*), FhuA, and FecA (the ferrichrome−Fe and citrate−Fe OMTs, respectively, in *E. coli*),

Table 4: Summary of the Data Presented in This Work[a]

Mutations	Pvd production	Pvd binding	Pvd motion	Pvd-^{55}Fe uptake	Pvd/Pvd-Fe exchange
G286C-L_1	*WT-phen.*	affected	*more mobile*	*WT-phen.*	*WT-phen.*
W362C-L_3	*WT-phen.*	affected	*more mobile*	*WT-phen.*	*WT-phen.*
W434C-L_4	-20%	affected	*more mobile*	-20%	affected
S603C-L_7	-20%	*WT-phen.*	*WT-phen*	+70%	*WT-phen.*
G701C-L_9	-20%	*WT-phen.*	*WT-phen*	-60%	affected
G794C-L_{11}	*WT-phen*	*WT-phen.*	*WT-phen*	*WT-phen*	*WT-phen.*

[a] The gray box corresponds to the only mutated residue within the siderophore binding site. The squares indicate the modified phenotypes. Pvd production was monitored by UV fluorescence assays in the extracellular medium. Pvd binding and motion in the FpvA mutants were studied by various techniques based on time-resolved fluorescence microscopy (Tables 1−3). Pvd−^{55}Fe uptake corresponds to the Pvd−^{55}Fe incorporation in the cells after 30 min (Figure 5). Finally Pvd/Pvd−Fe exchange was followed by FRET (Figure 6). WT-phen.: wild-type phenotype.

binds the apo and ferric forms of its siderophore at the same site. This property seems to be common to many siderophore OMTs and to hemoprotein OMTs, such as HasR (*43*). According the time-resolved fluorescence spectroscopy studies presented here (time-resolved fluorescence emission parameters (Table 1), fluorescence anisotropy decay parameters (Table 2), and iodide quenching parameters (Table 3)), the binding of metal-free Pvd to FpvA was affected in three mutants: G286C, W362C, and W434C. Only the W362 in loop L_3 belongs to the Pvd binding site. This residue is located very close to Pvd, within 4 Å (*9*, *10*). G286 is in the L_1 loop, far from the Pvd moiety, and W434 is in the L_4 loop, ~10 Å from the Pvd chromophore. For these three mutations, the iron-free siderophore was less tightly bound to its binding site and it was also more mobile and more solvent accessible than with wild-type FpvA. Moreover, for FpvA(W362C), an additional fluorescence lifetime was observed, indicating that this mutated FpvA and the chromophore moiety of Pvd differed from those for the wild-type FpvA−Pvd complex. These data are not surprising because W362 is part of the siderophore-binding site.

W434 affects the apo-siderophore binding (Tables 1−3). This residue, which, unlike W362, does not interact directly with Pvd, is located in loop L_4 and helps to stabilize the conformation of this loop as observed in the crystal structure (*9*, *10*). The bulky W434 side chain interacts with several atoms of the surrounding residues in loop L_4, and the W434C mutation strongly decreases the steric constraints imposed by this indole ring. This substitution may increase the flexibility of loop L_4. Residues of the β_7 and β_8 strands connected by loop L_4 are involved in binding Pvd. The W434C mutation may therefore have an effect on the conformation of loop L_4 and, therefore, on the conformation of the siderophore binding site and its interaction with metal-free Pvd.

G286C is the last residue of strand β_1 and is located far from the Pvd binding site. Strand β_1 interacts with strand β_{22}, the last β-strand of the barrel. Interactions between these two β-strands close the barrel. The replacement of a nonbulky residue, such as glycine, by a cysteine residue could modify the structure around the mutated site. The G286C mutation causes steric hindrance, due to the presence of a nonpolar hydrophobic cysteine sulfhydryl group, potentially disturbing interactions between the β_1 and β_{22} strands. This region and, indeed, this residue may therefore be important for the correct folding of FpvA. Moreover, the β_{21} and β_{22} strands are connected by loop L_{11}, which contains the Phe795 and Tyr796 residues of the Pvd binding site. Destabilization of the β_{22} strand due to the G286C mutation may slightly disturb the interactions between Phe795, Tyr796, and Pvd. In FpvA(G286C), the protein may be slightly misfolded in the area surrounding loop L_{11}, resulting in Pvd being less tightly bound to its binding site. However, this misfolding cannot be particularly severe, as this mutant transported ^{55}Fe as efficiently as the wild type (Figure 5) and as it has a stability in urea equivalent to wild-type FpvA (Figure 4).

Pvd−Fe Uptake. Time-resolved fluorescence spectroscopy could not be used to investigate the properties of Pvd−Fe binding to FpvA, because Pvd−Fe is not fluorescent. However, information about the effect of the mutations on Pvd−Fe binding properties and uptake into *P. aeruginosa* cells could be gleaned from the iron uptake data. FpvA(G286C) (loop L_1), FpvA(W362C) (loop L_4), FpvA(S603C) (loop L_7), and FpvA(G794C) (loop L_{11}) displayed ^{55}Fe incorporation at least as efficient as that with the wild-type FpvA (Figure 5). All four mutants completed at least two of the major steps involved in Pvd−Fe uptake: exchange of Pvd for Pvd−Fe on the FpvA binding site (decrease in fluorescence in Figures 6B and 6C) and recycling of Pvd on FpvA after iron release (increase in fluorescence in Figures 6B and 6C). The kinetics of these two steps were the same for these four mutants and for wild-type FpvA. However, higher-amplitude FRET signals were observed for FpvA(S603C) (loop L_7) and FpvA(G794C) (loop L_{11}) (Figure 6C). The conformation of FpvA loaded with recycled Pvd_{recycl} (FpvA−Pvd_{recycl}) must be slightly different for these two mutants, such that the efficiency of FRET between the Trp residues of FpvA and the Pvd chromophore is higher. Interestingly, the replacement of W362 by an alanine residue compromises Pvd−^{55}Fe binding and uptake (*44*), whereas its replacement by a cysteine residue had no effect.

For FpvA(G701C) (loop L_9) and FpvA(W434C) (loop L_4), which incorporated smaller amounts of ^{55}Fe than the wild type, only a decrease in fluorescence corresponding to the formation of FpvA−Pvd−Fe was observed, with no Pvd recycling on FpvA (Figure 6D). These mutants were loaded with Pvd−Fe, but the loading kinetics were very different from those for the wild-type receptor: slower, Pvd−Fe concentration-dependent and biphasic, with a fast first step and a slower second step. Previous binding studies of Pvd−Ga to wild-type FpvA have shown also biphasic kinetics: the bimolecular step (association of the ligand with the receptor) was followed by a slower step that presumably led to a more stable complex (*11*). The most likely explanation for this second step is that the binding of the ligand to the wild-type FpvA (*11*) or to the FpvA mutants (present study) induces a conformational change of the transporter. Further studies will be necessary to elucidate if this second step in the binding kinetic corresponds to a change of conformation of some extracellular loops. Since the kinetics in Figure 6D were slower compared to the other kinetics presented in

Figure 6, these data suggest also that FpvA(G701C) and FpvA(W434C) have lower affinity for Pvd−Fe. Following loading of the mutated FpvA with Pvd−Fe, transport occurred, but less efficiently than for the wild type, as less Pvd−^{55}Fe was incorporated into the cells (Figure 5). Surprisingly, absolutely no Pvd recycling on FpvA was observed (Figure 6D), suggesting either that Pvd recycling involves FpvA and these mutants were unable to carry out this process or that Pvd recycling occurs only when all the Pvd−Fe required has been transported into the periplasm. Further studies are required to improve our understanding of this complex step of Pvd recycling and to identify the precise step affected by the G701C and W434C mutations.

Surprisingly, the S603C mutation increased the amount of ^{55}Fe within the cells. No such phenotype has ever previously been described for a siderophore OMT. The most likely explanation is that S603 (loop L_7) may be important for the closing of the first gate and/or the translocation of Pvd−Fe across FpvA. The replacement of this residue by a cysteine may increase the efficiency of Pvd−Fe uptake. In FecA, this loop is involved in closing the citrate−Fe binding site before substrate uptake (*16*).

The Two-Gated System. A two-gated mechanism for ferric-siderophore uptake involves a change in the conformation of the extracellular loops after Pvd−Fe binding to FpvA, trapping Pvd−Fe in its binding site, followed by the opening of the second gate (plug domain). According to the phenotypes observed for the mutants studied here (Table 4), W434, S603, and G701 must be involved in the opening or closing of one of these gates. These three residues are located in the extracellular loops of FpvA (L_4 for W434, L_7 for S603, and L_9 for G701), suggesting that they probably play an important role in the closing of the first gate (extracellular loops). Glycine is a flexible residue, which can easily accommodate its Phi and Psi main chain angles, whereas tryptophan is a bulky residue involved in the geometric constraints of a loop conformation in FpvA. In the W434C and G701C mutants, either the first gate cannot close or the conformations of loops L_4 and L_9 do not allow Pvd−Fe uptake to occur normally. Moreover, other residues of loop L_4 may be involved in Pvd binding, and W434C may simply have an indirect effect on the conformation of the binding site.

S603 also seems to be involved in the closing of this first gate, but the S603C mutation increases the efficiency of Pvd−Fe uptake (Figure 5). FpvA may adopt a conformation increasing its ability to transport iron. S603 is part of loop L_7. The deletion of this loop in FhuA (*20*), FepA (*18*), or FecA (*45*) abolishes iron uptake, whereas only a large movement of loop L_7 and L_8 upon binding of the ferric-siderophore is observed in FecA (*16*).

Based on outer membrane transporter sequence alignments and the structures of FhuA, FepA, FecA, FpvA, and FptA, the extracellular loops are very specific for each transporter in terms of sequence and conformation. Almost nothing is known about conformational changes in these extracellular loops *in vivo*, except that loop L_7 seems to move in FhuA (*20*), FepA (*18*), FecA (*45*), and FpvA (Table 4 and Figures 5 and 6) in response to substrate binding. The motion of the other loops may be more complex and specific to each transporter, as deletion of the various extracellular loops in FhuA (*20*), FepA (*18*), and FecA (*45*) gave different phenotypes.

Does this two-gated system also work with the binding of apo-Pvd? Interestingly, two of the residues (S603 and G701) apparently involved in closing the first gate during Pvd−Fe uptake had no effect on the apo-Pvd binding (Tables 1−3). The structure analyses of FpvA loaded with Pvd or Pvd−Fe (*9*, *10*) and FecA loaded with apo-dicitrate or ferric-dicitrate (*16*) showed that both forms of the siderophore bind to a common binding site on the transporter (*9*, *16*, *46*). However, previous studies have already clearly shown that apo-Pvd binding involves a mechanism very different from that involved in binding of the ferric form (*11*, *21*). Pvd−metal binds much more rapidly with FpvA than the apo form (*11*). In addition, once bound to FpvA, Pvd−metal (the experiments had been carried out with Pvd−Ga) is less accessible to the aqueous solvent in its binding site than apo-Pvd, less mobile, and has an environment less polar (*21*). These data indicate that Pvd−metal is more trapped in its binding site than apo-Pvd. Since both forms of Pvd have the same binding site, Pvd−Fe or Pvd−Ga can only be trapped in its binding site because of a change of conformation of some extracellular loops. This change of conformation of the transporter is apparently absent for the apo Pvd binding to FpvA.

The present data, previous time-resolved fluorescence spectroscopy studies on FpvA−Pvd−Ga (*21*), the structures of unloaded FecA (the dicitrate−Fe OMT in *E. coli*) and FecA loaded with apo- and ferric-siderophore (*15*, *16*), and functional studies on FepA (the enterobactin−Fe OMT in *E. coli*) (*17*−*19*) and FhuA (*20*) suggest that a two-gated system controls uptake of siderophore−Fe. Moreover, in the case of the FpvA/Pvd system, the two-gated system seems to work for the ferric form and not for the apo form of the siderophore.

Pvd Production. The W434C, S603C, and G701C mutations decreased Pvd production by 20%. These mutations also modified uptake phenotype (decrease in Pvd−^{55}Fe incorporation for W434C and G701C and increase in Pvd−^{55}Fe incorporation for S603C, Figure 5). Despite the low diminution of Pvd production (20%), a parallel seems to exist between Pvd−Fe binding and/or uptake and signal transduction. Interestingly no such parallel seems to exist between the binding of apo-Pvd and Pvd production. Indeed, the W434C mutation affected the apo-Pvd binding and production, whereas the G701C and S603C mutations affected Pvd production but not apo-Pvd binding. These data suggest that the binding of Pvd−Fe, rather than of apo Pvd, probably induces regulation of the genes involved in iron uptake in *P. aeruginosa*.

In conclusion, we have presented here a first characterization of the phenotypes generated by the mutations G286C, W362C, W434C, G794C, S603C, and G701C (Figure 2). Our data suggest that W434, S603C, and G701C are involved in iron uptake and in the closing of the extracellular loops over Pvd−Fe, after binding to FpvA. This closing of the extracellular loops does not seem to be involved in the binding of metal-free Pvd. The apo and ferric forms of Pvd bind to FpvA via two different mechanisms, as suggested by previous FRET-based studies (*11*, *21*). Finally, our data also suggest a parallel between Pvd−Fe uptake and the regulation of Pvd production. Clearly more work will be necessary to confirm these first data. One of the next steps will be to express these mutants in a Pvd-deficient mutant, so that these receptors can be labeled with a fluorescent probe

or a spin marker (EPR studies) to investigate the conformation changes occurring in these extracellular loops during Pvd-Fe uptake.

REFERENCES

1. Abdallah, M. A., and Pattus, F. (2000) Siderophores and Iron-transport in Microorganisms, *J. Chin. Chem. Soc. 47*, 1−20.
2. Boukhalfa, H., and Crumbliss, A. L. (2002) Chemical aspects of siderophore mediated iron transport, *Biometals 15*, 325−339.
3. Braun, V. (2003) Iron uptake by *Escherichia coli*, *Front. Biosci. 8*, s1409−s1421.
4. Postle, K., and Kadner, R. J. (2003) Touch and go: tying TonB to transport, *Mol. Microbiol. 49*, 869−882.
5. Wiener, M. C. (2005) TonB-dependent outer membrane transport: going for Baroque?, *Curr. Opin. Struct. Biol. 15*, 394−400.
6. Demange, P., Wendenbaum, S., Linget, C., Mertz, C., Cung, M. T., and Dell, A., Abdallah, M. A. (1990) Bacterial siderophores: structure and NMR assigment of pyoverdins PaA, siderophores of *Pseudomonas aeruginosa* ATCC 15692, *Biol. Met. 3*, 155−170.
7. Schalk, I. (2006) *New insights on the iron metabolism in pathogenic Pseudomonas*, Vol. 4, pp 1−34, Kluwer Publishers, Dordrecht, The Netherlands.
8. Albrecht-Gary, A. M., Blanc, S., Rochel, N., Ocacktan, A. Z., and Abdallah, M. A. (1994) Bacterial iron transport: coordination properties of pyoverdin PaA, a peptidic siderophore of *Pseudomonas aeruginosa*, *Inorg. Chem. 33*, 6391−6402.
9. Cobessi, D., Célia, H., Folschweiller, N., Schalk, I. J., Abdallah, M. A., and Pattus, F. (2005) The crystal structure of the pyoverdin outer membrane receptor FpvA from *Pseudomonas aeruginosa* at 3.6 Å resolution, *J. Mol. Biol. 34*, 121−134.
10. Wirth, C., Meyer-Klaucke, W., Pattus, F., and Cobessi, D. (2007) From the periplasmic signaling domain to the extracellular face of an outer membrane signal transducer of *Pseudomonas aeruginosa*: Crystal structure of the ferric pyoverdine outer membrane receptor, *J. Mol. Biol. 68*, 398−406.
11. Clément, E., Mesini, P. J., Pattus, F., Abdallah, M. A., and Schalk, I. J. (2004) The binding mechanism of pyoverdin with the outer membrane receptor FpvA in *Pseudomonas aeruginosa* is dependent on its iron-loaded status, *Biochemistry 43*, 7954−7965.
12. Schalk, I. J., Hennard, C., Dugave, C., Poole, K., Abdallah, M. A., and Pattus, F. (2001) Iron-free pyoverdin binds to its outer membrane receptor FpvA in *Pseudomonas aeruginosa*: a new mechanism for membrane iron transport, *Mol. Microbiol. 39*, 351−360.
13. Greenwald, J., Hoegy, F., Nader, M., Journet, L., Mislin, G. L. A., Graumann, P. L., and Schalk, I. J. (2006) Real-time FRET visualization of ferric-pyoverdine uptake in *Pseudomonas aeruginosa*: a role for ferrous iron, *J. Biol. Chem. 282*, 2987−2995.
14. Schalk, I. J., Abdallah, M. A., and Pattus, F. (2002) Recycling of pyoverdin on the FpvA receptor after ferric pyoverdin uptake and dissociation in *Pseudomonas aeruginosa*, *Biochemistry 41*, 1663−1671.
15. Ferguson, A. D., Chakraborty, R., Smith, B. S., Esser, L., van der Helm, D., and Deisenhofer, J. (2002) Structural basis of gating by the outer membrane transporter FecA, *Science 295*, 1715−1719.
16. Yue, W. W., Grizot, S., and Buchanan, S. K. (2003) Structural evidence for iron-free citrate and ferric citrate binding to the TonB-dependent outer membrane transporter FecA, *J. Mol. Biol. 332*, 353−368.
17. Annamalai, R., Jin, B., Cao, Z., Newton, S. M., and Klebba, P. E. (2004) Recognition of ferric catecholates by FepA, *J. Bacteriol. 186*, 3578−3589.
18. Newton, S. M., Igo, J. D., Scott, D. C., and Klebba, P. E. (1999) Effect of loop deletions on the binding and transport of ferric enterobactin by FepA, *Mol. Microbiol. 32*, 1153−1165.
19. Scott, D. C., Newton, S. M., and Klebba, P. E. (2002) Surface loop motion in FepA, *J. Bacteriol. 184*, 4906−4911.
20. Endriss, F., and Braun, V. (2004) Loop deletions indicate regions important for FhuA transport and receptor functions in *Escherichia coli*, *J. Bacteriol. 186*, 4818−4823.
21. Folschweiller, N., Gallay, J., Vincent, M., Abdallah, M. A., Pattus, F., and Schalk, I. J. (2002) The interaction between pyoverdin and its outer membrane receptor in *Pseudomonas aeruginosa* leads to different conformers: a time-resolved fluorescence study, *Biochemistry 41*, 14591−14601.
22. Gumbart, J., Wiener, M. C., Tajkhorshid, E. (2007) Mechanics of force propagation in TonB-dependent outer membrane transport, *Biophys. J. 93*, 496−504.
23. Sansom, M. S. (1999) Membrane proteins: A tale of barrels and corks, *Curr. Biol. 9*, R254−257.
24. Ma, L., Kaserer, W., Annamalai, R., Scott, D. C., Jin, B., Jiang, X., Xiao, Q., Maymani, H., Massis, L. M., Ferreira, L. C., Newton, S. M., and Klebba, P. E. (2007) Evidence of ball-and-chain transport of ferric enterobactin through FepA, *J. Biol. Chem. 282*, 397−406.
25. Schons, V., Atkinson, R. A., Dugave, C., Graff, R., Mislin, G. L., Rochet, L., Hennard, C., Kieffer, B., Abdallah, M. A., and Schalk, I. J. (2005) The structure-activity relationship of ferric pyoverdine bound to its outer membrane transporter: implications for the mechanism of iron uptake, *Biochemistry 44*, 14069−14079.
26. Visca, P., Leoni, L., Wilson, M. J., and Lamont, I. L. (2002) Iron transport and regulation, cell signalling and genomics: lessons from *Escherichia coli* and *Pseudomonas*, *Mol. Microbiol. 45*, 1177−1190.
27. Beare, P. A., For, R. J., Martin, L. W., and Lamont, I. L. (2003) Siderophore-mediated cell signalling in *Pseudomonas aeruginosa*: divergent pathways regulate virulence factor production and siderophore receptor synthesis, *Mol. Microbiol. 47*, 195−207.
28. Lamont, I. L., Beare, P. A., Ochsner, U., Vasil, A. I., and Vasil, M. L. (2002) Siderophore-mediated signaling regulates virulence factor production in *Pseudomonas aeruginosa*, *Proc. Natl. Acad. Sci. U.S.A. 99*, 7072−7077.
29. Redly, G. A., and Poole, K. (2003) Pyoverdine-mediated regulation of FpvA synthesis in *Pseudomonas aeruginosa*: involvement of a probable extracytoplasmic-function sigma factor, FpvI, *J. Bacteriol. 185*, 1261−1265.
30. Redly, G. A., and Poole, K. (2005) FpvIR control of fpvA ferric pyoverdine receptor gene expression in *Pseudomonas aeruginosa*: demonstration of an interaction between FpvI and FpvR and identification of mutations in each compromising this interaction, *J. Bacteriol. 187*, 5648−5657.
31. Shen, J., Meldrum, A., and Poole, K. (2002) FpvA receptor involvement in pyoverdine biosynthesis in *Pseudomonas aeruginosa*, *J. Bacteriol. 184*, 3268−3275.
32. Wilson, M. J., and Lamont, I. L. (2000) Characterization of an ECF sigma factor protein from *Pseudomonas aeruginosa*, *Biochem. Biophys. Res. Commun. 273*, 578−583.
33. Wilson, M. J., McMorran, B. J., and Lamont, I. L. (2001) Analysis of promoters recognized by PvdS, an extracytoplasmic-function sigma factor protein from *Pseudomonas aeruginosa*, *J. Bacteriol. 183*, 2151−2155.
34. Braun, V., Mahren, S., and Ogierman, M. (2003) Regulation of the FecI-type ECF sigma factor by transmembrane signalling, *Curr. Opin. Microbiol. 6*, 173−180.
35. Koster, M., van Klompenburg, W., Bitter, W., Leong, J., and Weisbeek, P. (1994) Role for the outer membrane ferric siderophore receptor PupB in signal transduction across the bacterial cell envelope, *EMBO J. 13*, 2805−2813.
36. Koster, M., van de Vossenberg, J., Leong, J., and Weisbeek, P. J. (1993) Identification and characterization of the pupB gene encoding an inducible ferric-pseudobactin receptor of *Pseudomonas putida* WCS358, *Mol. Microbiol. 8*, 591−601.
37. Dean, C. R., and Poole, K. (1993) Expression of the ferric enterobactin receptor (PfeA) of *Pseudomonas aeruginosa*: involvement of a two-component regulatory system, *Mol. Microbiol. 8*, 1095−1103.
38. Morales, V. M., Backman, A., and Bagdasarian, M. (1991) A series of wide-host-range low-copy-number vectors that allow direct screening for recombinants, *Gene 97*, 39−47.
39. Poole, K., Neshat, S., and Heinrichs, D. (1991) Pyoverdine-mediated iron transport in *Pseudomonas aeruginosa*: involvement of a high-molecular-mass outer membrane protein, *FEMS Microbiol. Lett. 62*, 1−5.
40. Figurski, D. H., and Helinski, D. R. (1979) Replication of an origin-containing derivative of plasmid RK2 dependent on a plasmid function provided in trans, *Proc. Natl. Acad. Sci. U.S.A. 76*, 1648−1652.
41. Ocaktan, A., Schalk, I., Hennard, C., Linget-Morice, C., Kyslik, P., Smith, A. W., Lambert, P. A., and Abdallah, M. A. (1996) Specific photoaffinity labelling of a ferripyoverdin outer membrane receptor of *Pseudomonas aeruginosa*, *FEBS Lett. 396*, 243−247.
42. Schalk, I. J., Kyslik, P., Prome, D., van Dorsselaer, A., Poole, K., Abdallah, M. A., and Pattus, F. (1999) Copurification of the FpvA

ferric pyoverdin receptor of *Pseudomonas aeruginosa* with its iron-free ligand: implications for siderophore-mediated iron transport, *Biochemistry 38*, 9357−9365.
43. Letoffe, S., Deniau, C., Wolff, N., Dassa, E., Delepelaire, P., Lecroisey, A., and Wandersman, C. (2001) Haemophore-mediated bacterial haem transport: evidence for a common or overlapping site for haem-free and haem-loaded haemophore on its specific outer membrane receptor, *Mol. Microbiol. 41*, 439−450.
44. Shen, J. S., Geoffroy, V., Neshat, S., Jia, Z., Meldrum, A., Meyer, J. M., and Poole, K. (2005) FpvA-mediated ferric pyoverdine uptake in *Pseudomonas aeruginosa*: identification of aromatic residues in FpvA implicated in ferric pyoverdine binding and transport, *J. Bacteriol. 187*, 8511−8515.
45. Sauter, A., and Braun, V. (2004) Defined inactive FecA derivatives mutated in functional domains of the outer membrane transport and signaling protein of *Escherichia coli* K-12, *J. Bacteriol. 186*, 5303−5310.
46. Cobessi, D., Celia, H., and Pattus, F. (2005) Crystal structure at high resolution of ferric-pyochelin and its membrane receptor FptA from *Pseudomonas aeruginosa*, *J. Mol. Biol. 352*, 893−904.
47. Kinosita, K., Jr., Kawato, S., and Ikegami, A. (1977) A theory of fluorescence polarization decay in membranes, *Biophys. J. 20*, 289−305.

BI700997W